

Investigation of enhancement in planar fast neutron detector efficiency with stacked structure using Geant4

Shivang Tripathi^{1,2} · Chandrakant Upadhyay² · C. P. Nagaraj² · K. Devan² · A. Venkatesan² · K. Madhusoodanan²

Received: 26 January 2017 / Revised: 25 May 2017 / Accepted: 2 June 2017 / Published online: 25 October 2017
© Shanghai Institute of Applied Physics, Chinese Academy of Sciences, Chinese Nuclear Society, Science Press China and Springer Nature Singapore Pte Ltd. 2017

Abstract Geant4 based Monte Carlo study has been carried out to assess the improvement in efficiency of the planar structure of Silicon Carbide (SiC)-based semiconductor fast neutron detector with the stacked structure. A proton recoil detector was simulated, which consists of hydrogenous converter, i.e., high-density polyethylene (HDPE) for generating recoil protons by means of neutron elastic scattering (n, p) reaction and semiconductor material SiC, for generating a detectable electrical signal upon transport of recoil protons through it. SiC is considered in order to overcome the various factors associated with conventional Si-based devices such as operability in a harsh radiation environment, as often encountered in nuclear facilities. Converter layer thickness is optimized by considering 10^9 neutron events of different monoenergetic neutron sources as well as ^{241}Am -Be neutron spectrum. It is found that the optimized thickness for neutron energy range of 1–10 MeV is $\sim 400 \mu\text{m}$. However, the efficiency of fast neutron detection is estimated to be only 0.112%, which is considered very low for meaningful and reliable detection of neutrons. To overcome this problem, a stacked juxtaposition of converter layer between SiC layers has been analyzed in order to achieve high efficiency. It is

noted that a tenfold efficiency improvement has been obtained—1.04% for 10 layers stacked configuration vis-à-vis 0.112% of single converter layer detector. Further simulation of the stacked detector with respect to variable converter thickness has been performed to achieve the efficiency as high as $\sim 3.85\%$ with up to 50 stacks.

Keywords Geant4 · Fast neutron detector · Silicon carbide · Recoil proton · Stacked detector

1 Introduction

Nuclear reactors, nuclear recycling, and reprocessing facilities often employ neutron detectors as monitoring and control sensor. Operating conditions in such nuclear facilities generally include harsh radiation environment associated with high gamma dose rate and temperature [1]. Thus, the neutron sensors for such facilities should be designed and manufactured so as to make them operable in harsh conditions. Self-powered neutron detectors (SPNDs) [2] and fission chambers (FCs) [3, 4] are quite popular for such application requirements. SPNDs have been used widely as in-core flux monitors in thermal reactors owing to the high cross sections of their emitter materials to the thermal neutrons [5, 6]. However, their sensitivity to both neutrons as well as γ -rays and delayed response for few emitters limits its operation [7]. On the other hand, FCs are good at gamma discrimination by virtue of high charge associated with extremely energetic fission fragments [8]. However, it is a gas-filled type detector that requires comparatively high voltage supply to collect the charge pairs. In addition, these detectors have other limitations viz. (a) high cost of enriching the fissile material in order to

This work was supported by the grant of a research fellowship from Indira Gandhi Centre for Atomic Research, Department of Atomic Energy, India.

✉ Shivang Tripathi
shivang@igcar.gov.in

¹ Homi Bhabha National Institute, Anushaktinagar, Mumbai 400094, India

² Indira Gandhi Centre for Atomic Research, Kalpakkam 603102, India

attain high efficiency [1] (b) inability to provide energy spectrum information [8] (c) large size. Therefore, there is a compelling need to conceive a detection system which could be employed as an alternative or diverse sensor of neutron detection having features—harsh environment operability, wide neutron spectrum response, and compact vis-à-vis gas-filled detectors. The wide energy spectrum response is expected to facilitate the study of shielding effectiveness of various materials as well as neutron detector efficiency calibration in a known spectrum. Further, miniaturization of the detector is targeted to ease the handling, installations; finding application where compact nuclear sensors are desirable such as space, nuclear reprocessing plants, and special nuclear material detection.

With above objective, we conceptualized a fast neutron detector, which can be exposed to a total neutron flux of the order of 10^{10} n/cm²s, a gamma field of 10 Gy/h and temperature not exceeding 100 °C—a typical ex-vessel location of a fast reactor. A wide band-gap semiconductor, Silicon Carbide (SiC) (3.25 eV for 4H-SiC polytype), has been chosen to study neutronic interaction properties under the above-stated conditions. The expected gamma dose at the ex-vessel location is quite less than the dose, which degrades the SiC detector performance or hinders its detection efficiency. High-density polyethylene (HDPE) (C₂H₄)_n has been employed as a converter material to generate recoil protons upon interaction with fast neutrons [9–15]. The details of fast neutron detection through proton recoil method and validation of our model with analytical method could be found in our previous work and references therein [10]. The present work focuses on the study of the improvement in efficiency of planar SiC-based semiconductor fast neutron detector with the stacked structure. Geant4 [16] simulations have been performed to optimize the converter layer thickness for different monoenergetic and ²⁴¹Am-Be neutron sources. Effect of low-level discriminator (LLD) on detection efficiency is analyzed. Also, stacked structure has been simulated to study the improvement in the detection efficiency.

2 A Geant4 simulation

Geant4 is a simulation tool kit for simulating the transport of particles through matter. It offers a complete range of functionality including tracking, geometry, physics models, and processes [17, 18]. It is capable of tracking down the secondary particles as well. It provides a vast set of well-defined physics models including hadronic, electromagnetic, and optical processes from low energy to very high energy range [19]. It has been developed with software engineering and object-oriented technology and implemented in C++ programming language.

2.1 Model description

The Geant4.10.00.p02 version is used to build the model. The planar detector geometry has been constructed using Geometry Category of Geant4. Geometry, as shown in Fig. 1a, consists of a converter layer of HDPE (density 0.94 g/cm³) with 1 cm × 1 cm front face (*XY*-plane), and thickness (*Z*-axis) is varied from one micrometer to few millimeters in order to optimize the thickness of converter layer. Here, optimized thickness represents the thickness at which the detector efficiency is maximum. In other words, the thickness at which, the maximum number of recoil protons will punch through the converter layer into the SiC semiconductor region to generate a detectable signal. Adjacent to the converter is a detector layer made up of SiC with similar *XY*-plane, and thickness is kept at 600 μm as shown in Fig. 1b. General particle source (GPS), class of particle category, has been utilized to generate a spectrum of the ²⁴¹Am-Be neutron source taken from the ISO Report 8529-1 [20]. It is positioned at 1 cm distance from the converter face. In practical applications, the neutron will not be generated in parallel beams rather fall in random directions on the detector. But in order to achieve maximum efficiency, the source is set such that neutrons will impinge perpendicularly and uniformly on the front face of the converter layer (in direction of *Z*-axis) as illustrated in Fig. 1b. Standard physics model QGSP_BERT_HP has been used, which employs high precision neutron model used for neutron below 20 MeV [21].

In order to optimize the converter thickness, five iterations of 10^9 neutrons have been simulated for different monoenergetic as well as ²⁴¹Am-Be neutron source. This special case of ²⁴¹Am-Be neutron source has been chosen to facilitate the laboratory-scale experiment of the detector with standard neutron source. Furthermore, five iterations would help in better convergence of results. After determining the optimum thickness, 10^9 neutrons have been fired to illustrate the energy deposition by recoil protons, other charged particles in converter and detector.

Furthermore, the number of converters and detectors has been increased to implement the stacked detector configuration as depicted in Fig. 1c, and enhancement in efficiency was estimated. Simulations were performed in GNU HPC clusters, and all physics processes were kept on so as to reflect the best practical situation. Dead layer and temperature effect were not considered in this work. It should be noted that these effects would further degrade the detection efficiency.

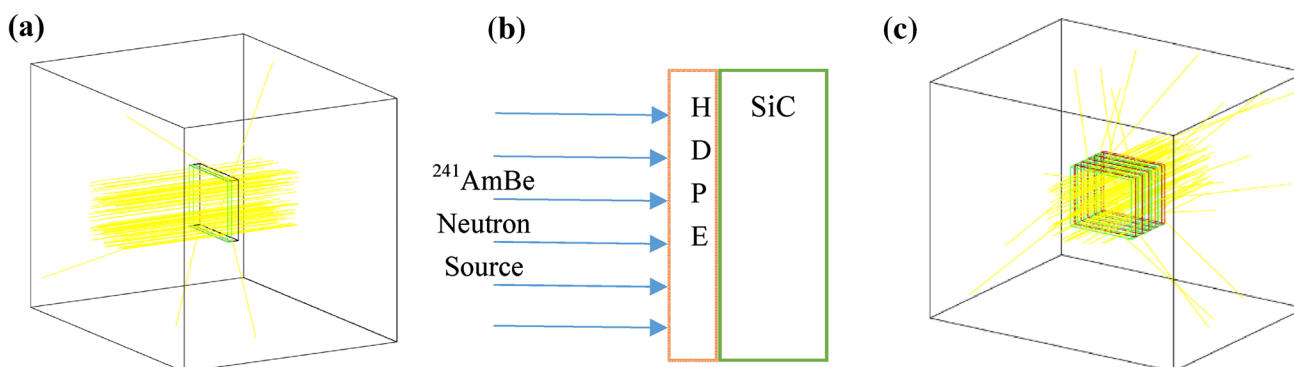


Fig. 1 a Visualization of Geant4 simulation of SiC detector with HDPE converter layer. Outer volume is mandatory mother volume; inside is detector geometry, and yellow line (online version) shows a

trajectory of neutrons passing through detector (b) planar diode detector schematic comprising of HDPE converter and SiC detector volume c stacked detector

3 Results and discussion

3.1 Nuclear interactions in HDPE converter

To determine the reactions that are taking place in the converter, a simulation was performed with 1 cm thick HDPE structure. It was irradiated by 10^6 neutrons of the $^{241}\text{Am-Be}$ neutron source. List of nuclear reactions along with the reaction Q -value is tabulated in Table 1.

Table 1 represents the reactions, which are happening in HDPE material upon interaction with the incident neutrons. It is evident that neutron reaction with hydrogen, i.e., (n, p) reaction is dominating ($\sim 72\%$), which is elastic scattering in nature. This is because, for fast neutrons, elastic scattering cross section is higher than other reaction cross sections. In addition to this, neutrons will also undergo elastic scattering reaction with Carbon nuclei, which is the next reaction in terms of dominance ($\sim 26\%$). Other than these reactions, neutron will also undergo several inelastic

scattering reactions with Carbon and Hydrogen nuclei [$^{12}\text{C}(n, n')^{12}\text{C}$; $^{12}\text{C}(n, n')^{13}\text{C}$; $^1\text{H}(n, n')^2\text{H}$] and a very few (n, α) reactions [$^{12}\text{C}(n, \alpha)^9\text{Be}$; $^{13}\text{C}(n, \alpha)^{10}\text{Be}$] due to very low cross section. Some reactions have negative Q -value, which shows these reactions will occur only when the incident neutrons will have energy equal to or greater than the threshold energy.

Table 2 shows the list of particles generated due to neutron interaction with HDPE along with their mean kinetic energy and range of the kinetic energies at the time of their production.

3.2 Nuclear interactions in SiC detector

Similar approach was adopted for simulating the nuclear interactions in SiC material. List of nuclear reactions along with the reaction Q -value is tabulated in Table 3.

From Table 3, it is evident that the elastic scattering reaction with Carbon and Silicon nuclei is dominant

Table 1 List of nuclear reactions in HDPE converter for 10^6 incident neutrons (where N is number of Gamma; $N = 1-4$)

Nuclear reactions	Frequency relative to total neutron interactions (%)	Q -value
$n + ^{12}\text{C} \rightarrow N \gamma + ^{13}\text{C}$	0.0010	186.34 keV
$n + ^{12}\text{C} \rightarrow N \gamma + \alpha + ^9\text{Be}$	0.1017	- 5.7038 MeV
$n + ^{12}\text{C} \rightarrow N \gamma + n + ^{12}\text{C}$	1.3493	- 290.49 eV
$n + ^{12}\text{C} \rightarrow \alpha + ^9\text{Be}$	0.1291	- 5.7012 MeV
$n + ^{12}\text{C} \rightarrow n + ^{12}\text{C}$	26.2475	144.32 eV
$n + ^{13}\text{C} \rightarrow N \gamma + \alpha + ^{10}\text{Be}$	0.0010	- 3.8386 MeV
$n + ^{13}\text{C} \rightarrow N \gamma + n + ^{13}\text{C}$	0.0131	- 230.71 eV
$n + ^{13}\text{C} \rightarrow \alpha + ^{10}\text{Be}$	0.0017	- 3.8353 MeV
$n + ^{13}\text{C} \rightarrow n + ^{13}\text{C}$	0.2885	- 28.831 keV
$n + ^1\text{H} \rightarrow N \gamma + ^2\text{H}$	0.0003	578.25 keV
$n + ^1\text{H} \rightarrow n + p$	71.8599	840.86 eV
$n + ^2\text{H} \rightarrow n + ^2\text{H}$	0.0064	429.84 eV

The total number of neutron interactions is 281,108. Negative Q -value indicates the threshold reactions

Table 2 List of generated particles in HDPE with their mean kinetic energy for 10^6 incident neutrons

Generated particles	Number	Mean kinetic energy	Range of kinetic energy
^{10}Be	8	1.4649 MeV	303.12 keV–2.7232 MeV
^9Be	649	1.1741 MeV	9.0611 keV–3.5147 MeV
^{12}C	77,577	409.14 keV	1.3303 eV–2.9667 MeV
^{13}C	851	360.36 keV	897.91 eV–2.5871 MeV
α	657	1.8154 MeV	206.39 keV–4.8089 MeV
^2H	19	1.5774 MeV	151.93 keV–5.3214 MeV
γ	10,607	1.6236 MeV	1.0013 keV–9.142 MeV
n	3830	2.2004 MeV	31.444 keV–6.1871 MeV
p	202,004	1.5502 MeV	1.0023 eV–10.726 MeV

Table 3 List of nuclear reactions in SiC material for 10^6 incident neutrons (where N is number of Gamma; $N = 1-8$)

Nuclear reactions	Frequency relative to total neutron interactions (%)	Q -value
$n + ^{12}\text{C} \rightarrow N \gamma + ^{13}\text{C}$	0.000427967	– 734.52 keV
$n + ^{12}\text{C} \rightarrow N \gamma + \alpha + ^9\text{Be}$	0.145080736	– 5.7038 MeV
$n + ^{12}\text{C} \rightarrow N \gamma + n + ^{12}\text{C}$	1.906164005	– 231.52 eV
$n + ^{12}\text{C} \rightarrow \alpha + ^9\text{Be}$	0.191729114	– 5.7012 MeV
$n + ^{12}\text{C} \rightarrow n + ^{12}\text{C}$	39.50347295	139.26 eV
$n + ^{13}\text{C} \rightarrow N \gamma + \alpha + ^{10}\text{Be}$	0.0012839	– 3.8359 MeV
$n + ^{13}\text{C} \rightarrow N \gamma + n + ^{13}\text{C}$	0.018402571	– 260.39 eV
$n + ^{13}\text{C} \rightarrow \alpha + ^{10}\text{Be}$	0.001711867	– 3.8358 MeV
$n + ^{13}\text{C} \rightarrow n + ^{13}\text{C}$	0.416839637	– 27.684 keV
$n + ^{28}\text{Si} \rightarrow N \gamma + ^{29}\text{Si}$	0.008987302	6.4167 MeV
$n + ^{28}\text{Si} \rightarrow N \gamma + \alpha + ^{25}\text{Mg}$	0.259775831	– 2.4198 MeV
$n + ^{28}\text{Si} \rightarrow N \gamma + n + ^{28}\text{Si}$	10.41585531	– 63.193 eV
$n + ^{28}\text{Si} \rightarrow N \gamma + p + ^{28}\text{Al}$	0.907289558	– 3.6085 MeV
$n + ^{28}\text{Si} \rightarrow \alpha + ^{25}\text{Mg}$	0.411276069	– 2.7349 MeV
$n + ^{28}\text{Si} \rightarrow n + ^{28}\text{Si}$	41.15028909	31.809 eV
$n + ^{28}\text{Si} \rightarrow p + ^{28}\text{Al}$	0.397581132	– 3.8759 MeV
$n + ^{29}\text{Si} \rightarrow N \gamma + 2 n + ^{28}\text{Si}$	0.000855934	– 1.149 MeV
$n + ^{29}\text{Si} \rightarrow N \gamma + \alpha + ^{26}\text{Mg}$	0.024394106	– 31.934 keV
$n + ^{29}\text{Si} \rightarrow N \gamma + n + ^{29}\text{Si}$	0.738242683	– 48.522 eV
$n + ^{29}\text{Si} \rightarrow N \gamma + p + ^{29}\text{Al}$	0.013694937	– 2.8964 MeV
$n + ^{29}\text{Si} \rightarrow \alpha + ^{26}\text{Mg}$	0.016690704	– 89.088 keV
$n + ^{29}\text{Si} \rightarrow n + ^{29}\text{Si}$	1.746104432	31.061 eV
$n + ^{29}\text{Si} \rightarrow p + ^{29}\text{Al}$	0.017118671	– 2.9129 MeV
$n + ^{30}\text{Si} \rightarrow N \gamma + ^{31}\text{Si}$	0.000427967	4.3037 MeV
$n + ^{30}\text{Si} \rightarrow N \gamma + \alpha + ^{27}\text{Mg}$	0.000855934	– 4.2002 MeV
$n + ^{30}\text{Si} \rightarrow N \gamma + n + ^{30}\text{Si}$	0.411704035	2.2936 keV
$n + ^{30}\text{Si} \rightarrow N \gamma + p + ^{30}\text{Al}$	0.000427967	– 6.8197 MeV
$n + ^{30}\text{Si} \rightarrow \alpha + ^{27}\text{Mg}$	0.001711867	– 4.2538 MeV
$n + ^{30}\text{Si} \rightarrow n + ^{30}\text{Si}$	1.29160372	25.478 eV

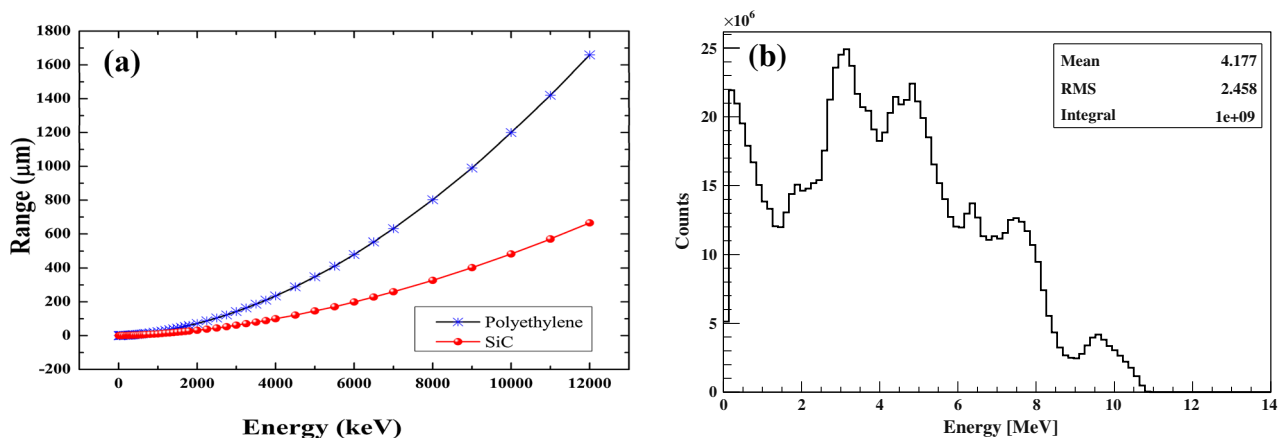
The total number of neutron interactions is 233663. Negative Q -value indicates the threshold reactions

with ~ 39 and $\sim 41\%$ reactions, respectively, in SiC, followed by inelastic scattering reaction with Si nuclei and other threshold reactions resulting in α -particles, Mg, Al, Be... as reaction products. The dominant reaction products

produced in SiC have lower energy range (Table 4) than the products generated in HDPE (Table 2). Therefore, an energetic reaction product generated in HDPE converter and transported to SiC, would deposit higher energy in SiC

Table 4 List of generated particles in SiC with their mean kinetic energy for 10^6 incident neutrons

Generated particles	Number	Mean kinetic energy	Range of kinetic energy
^{28}Al	3049	367.77 keV	16.171 keV–1.1204 MeV
^{29}Al	72	349.65 keV	28.833 keV–1.0893 MeV
^{30}Al	1	581.19 keV	581.19 keV–581.19 keV
^{10}Be	7	1.2123 MeV	160.58 keV–2.1968 MeV
^9Be	787	1.1595 MeV	14.152 keV–3.137 MeV
^{12}C	96,759	395.14 keV	0.34078 eV–2.9473 MeV
^{13}C	1018	347.16 keV	180.32 eV–2.4177 MeV
^{25}Mg	1568	876.6 keV	43.409 keV–2.3849 MeV
^{26}Mg	96	928.07 keV	110.96 keV–2.0859 MeV
^{27}Mg	6	788.25 keV	194.37 keV–1.5206 MeV
^{28}Si	120,493	145.37 keV	0.26237 eV–1.3631 MeV
^{29}Si	5826	154.35 keV	15.233 eV–1.1235 MeV
^{30}Si	3980	139.39 keV	2.4636 eV–1.1573 MeV
^{31}Si	1	70.041 keV	70.041 keV–70.041 keV
α	2464	3.428 MeV	197.08 keV–8.2182 MeV
γ	49,939	1.5854 MeV	406.57 eV–8.9998 MeV
n	31,526	2.9368 MeV	6.335 keV–9.4629 MeV
p	3122	3.153 MeV	238.19 keV–7.5591 MeV

**Fig. 2** **a** Range of protons in HDPE and SiC computed using SRIM. **b** Spectrum of ^{241}Am -Be neutron source generated using Geant4

in comparison with the products generated in SiC itself, provided, the thickness of converter is optimized. Thereby, a HDPE converter layer over SiC detector will result in a better detection efficiency and detectable signal. Franceschini et al. [22] have also reported a better detection efficiency in the presence of converter layer over SiC detector.

In Table 4, one can see that significant number of γ -rays is also generating due to various inelastic scatterings and other reactions. Also, neutron fields are generally accompanied with γ -background. These γ -rays can undergo photoelectric, Compton interactions with atomic electrons, and it can also be converted into an electron–positron pair, but it would hardly affect the operation of the SiC detector as it has been reported that change in SiC-based detector

response is negligible even after 22.7 MGy exposure to γ -rays [23].

3.3 Optimization of HDPE converter thickness for wide energy range of neutrons

The recoil proton generated in converter will tend to lose its energy continuously along the path, which limits its range in the material. Figure 2a shows the range of proton in HDPE and SiC computed using SRIM [24]. It is evident that 1 MeV proton can traverse up to 20 μm while 10 MeV proton up to 1200 μm . In spite of the fact that having a HDPE converter of around 9 cm will result in approximately 99% neutron interactions [10], we could not employ

a converter of such thickness because most of the recoil protons will be stopped in converter itself, before reaching the SiC detector volume. Thus, Geant4 simulation has been performed to optimize the HDPE converter thickness for different neutron energies ranging from 0.5 to 10 MeV and a special case of ^{241}Am -Be neutron source spectrum as shown in Fig. 2b. The optimized thickness is the thickness at which the maximum number of recoil protons is detected. It is assumed that each recoil proton, reaching the detector with sufficient energy, will give a detectable signal, i.e., proton detection efficiency is 100%. About 10^9 neutron events have been simulated 5 times to determine the detector's absolute efficiency, i.e., number of recoil protons reaching SiC detector volume divided by total incident neutrons [25].

Figure 3a depicts the detector efficiency for different energy neutrons and different converter thicknesses. It could be observed that after a certain thickness of converter, efficiency is decreasing. This is due to the self-absorption of proton energy in converter itself. This self-absorption limits the efficiency of the planar detector. Since, neutrons of different energies provide maximum efficiency for different thickness, there is a need to select a thickness, which could be efficient for a specific energy range that is 0.5–11 MeV in the context of this work. Therefore, in order to accommodate a wide energy range of neutrons, we have considered 400 μm thickness as an optimized one in this work.

From Fig. 3a, the optimized HDPE converter thickness for different monoenergetic neutron source can also be chosen. For example, a thickness of 100 μm can be selected as an optimized thickness for a 2.5 MeV D-T neutron source. Similarly, for an application which requires 10 MeV neutrons to be detected, a converter layer of ~ 1.1 mm should be considered as an optimum one. Further, a special case has been taken to optimize the HDPE thickness for ^{241}Am -Be neutron source and illustrated in Fig. 3b. It is apparent that for thicknesses of HDPE converter ranging from 400 to 1000 μm , the detector will provide maximum efficiency of 0.112–0.117%.

Thus, we can say that for the thickness of 400–1000 μm , detector efficiency is approximately constant. It should be noted that there are relatively few neutrons significantly higher than 6 MeV in the ^{241}Am -Be spectrum. Also, the larger thickness would restrict the number of recoil protons reaching the detector. Thus, to cover the wide range of specified source spectrum, a 400 μm thickness could be regarded as the optimum thickness, which is well in agreement with the optimum result for the 6 MeV monoenergetic neutron source obtained in Fig. 3a. The efficiency of neutron detector with 400 μm thick HDPE converter with respect to different monoenergetic neutron

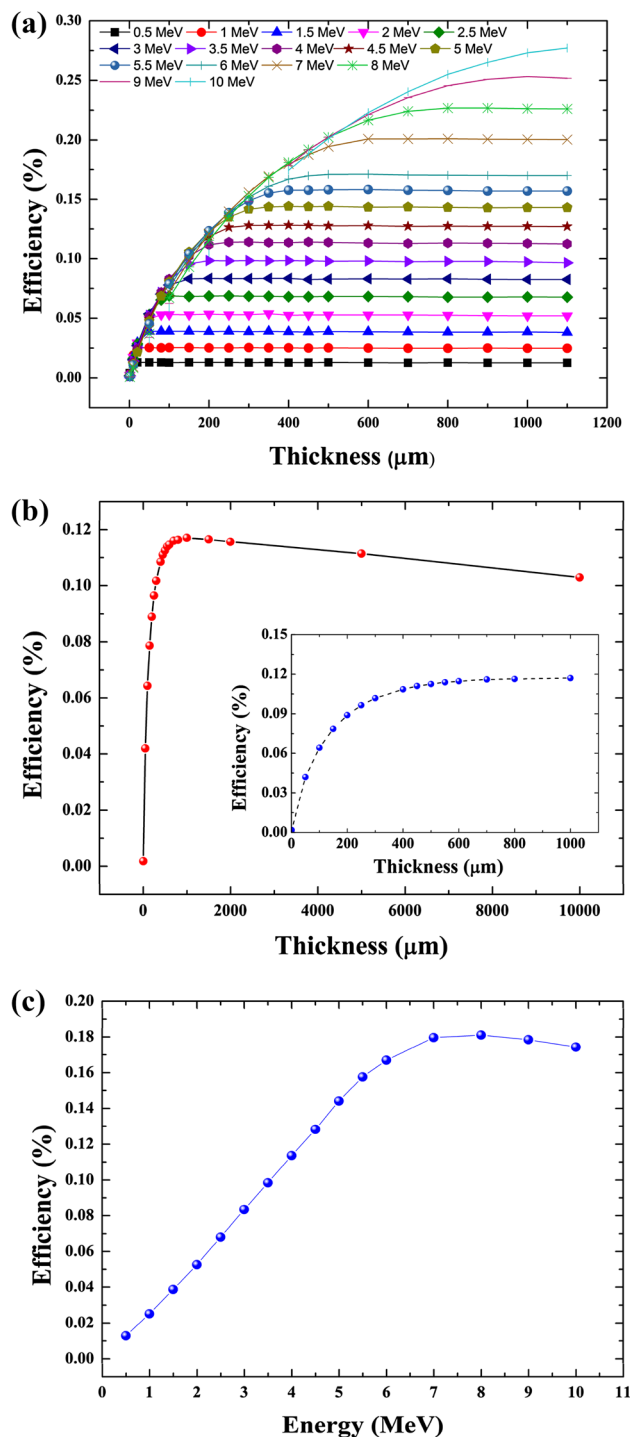


Fig. 3 a Optimization of converter thickness for different energy neutron. b Detector efficiency as a function of HDPE converter thickness for ^{241}Am -Be neutron source. (Inset: Zoomed view of plot from origin to 1000 μm thickness). c Efficiency of neutron detector with 400 μm thick HDPE converter for different monoenergetic neutron sources

source is illustrated in Fig. 3c. It can be observed that with 400 μm thick HDPE converter, maximum efficiency of $\sim 0.18\%$ can be achieved for up to 7 MeV

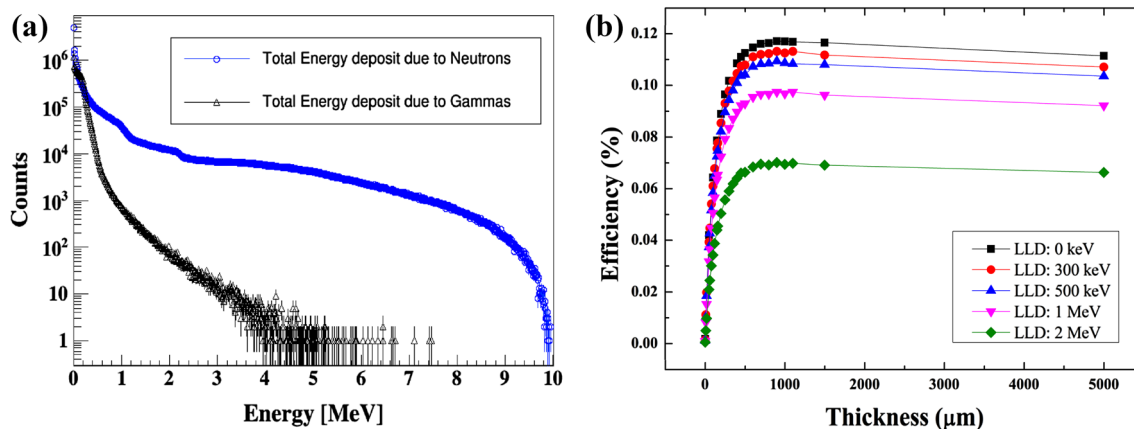


Fig. 4 **a** Comparison of energy deposition due to neutron and gamma events in SiC. **b** Effect of LLD on SiC detector efficiency

monoenergetic neutron source. For neutron energies higher than 7 MeV, efficiency is decreasing since the optimized value of HDPE thickness is higher than 400 μm , for high energy neutron sources as shown in Fig. 3a.

3.4 Calculation of optimum thickness of SiC for $^{241}\text{AmBe}$ neutron source

For $^{241}\text{Am-Be}$ neutron source, maximum recoil energy of proton that can be generated in HDPE is 10.726 MeV (Table 2). The range of proton in SiC is computed using SRIM code, and it is found to be approximately 571 μm for a proton of energy 11 MeV (Fig. 2a). Thus, to allow the maximum recoil proton to deposit all of its energy in detector volume, the thickness of the SiC detector active volume is chosen to be 600 μm .

3.5 Simulation of SiC detector in mixed neutron-gamma field

The primary concern of neutron detector in a mixed neutron-gamma field is the inability of the detector to accurately discriminate between the two. Also, a significant number of γ -rays are being generated along with the other charged particles in SiC as well as in HDPE converter. Therefore, to analyze the effect of gamma background over neutron detection, a simulation was performed with gamma and neutron source of energies ranging from 100 keV to 10 MeV with 10^9 particles. Figure 4a represents the comparison of their energy deposition in SiC detector. Gammas would generally undergo photoelectric effect at low energy region while Compton scattering and pair production at high energy region. Pair production reaction generally occurs when the incident gamma energy is > 1.02 MeV. On the other hand, neutron induced events are mainly due to the energy deposited by recoil protons generated in converter layer. It is evident that such a heavy gamma

background signals would be comparable to neutron signals below 1 MeV range. Between 1 and 2 MeV, there would be gamma effect on neutron signals, which could be easily distinguishable and can be discriminated with the pulse height spectrum or by applying low-level discriminator (LLD). Beyond 3 MeV, there is a very minimal effect of gamma events, which could be neglected in case of fast neutrons.

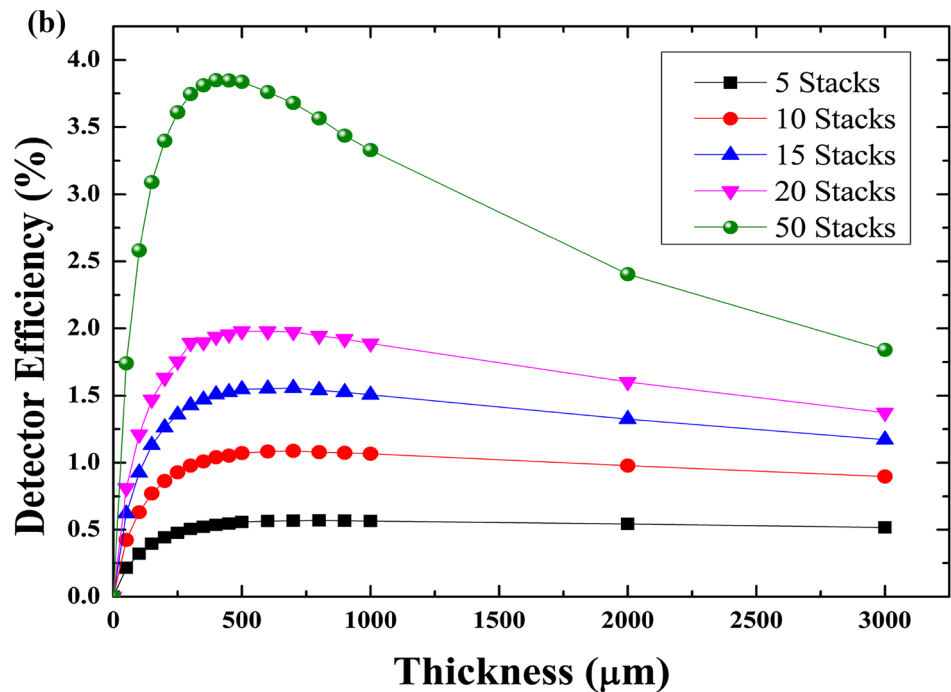
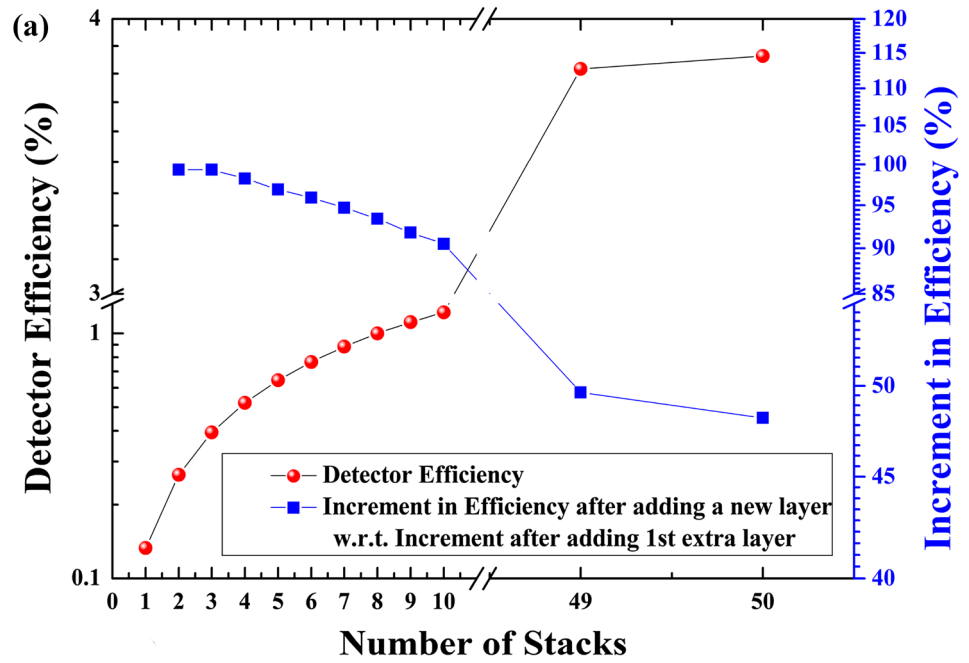
Figure 4b shows the effect of LLD on detector efficiency. As can be seen, simply increasing the LLD to higher values can limit the background radiation, as from γ -rays and other charged particles, but at the same time, some proton recoil events will inevitably be discriminated, because the proton recoil energy distribution extends all the way to zero. Therefore, the detector with a finite discrimination level will always have a slightly lower efficiency.

The efficiency achieved with this proton recoil detector is very small. However, for a reliable and consistent monitoring, this kind of detector efficiency is often regarded as unacceptably low. Therefore, to enhance the efficiency of the detector, with major characteristics unaffected, a special configuration consisting several layers of converters and active SiC layers (stacked configuration), as shown in Fig. 1c, has been considered and assessed.

3.6 Stacked detector simulation

Converter and detector volume is regarded as a single layer, and by using the G4Replica Class of Geant4, it is replicated in order to generate stacked structure as shown in Fig. 1c. The optimum value of thickness is used for converter and detector, i.e., 400 μm for HDPE and 600 μm for SiC. Simulations have been performed for 10^9 neutron events and up to 10 layers. Efficiency, as defined previously, is estimated by increasing the number of layers in the stack. From Fig. 5a, it is apparent that as we increase the number of stacks, efficiency will also increase but not

Fig. 5 **a** Increment in efficiency of SiC-based detector with layers in the stack. Percentage increment in efficiency upon increasing the number of layers. **b** Efficiency variation with respect to converter thickness for a stacked detector with 5, 10, 15, 20, and 50 stacks



linearly. As we increase the number of layers from 1 to 2, the increment in efficiency is almost double, i.e., 99.33% increment. Further, from second-layer to third-layer increment is ~ 99% of the first increment. From third- to fourth-layer increment is ~ 98.22% of the first increment. Similarly, from ninth-layer to tenth-layer increment is ~ 90.49% of the first increment. Thus, it appears that adding the 10th layer is approximately the same increase in total detection as adding the 2nd layer. Further addition of

50th layer offers only ~ 48% increment in efficiency to what we achieved by adding a 2nd layer. It shows that after a certain number of layers efficiency will saturate. This is due to the fact that probability of interaction for neutron with HDPE will saturate at certain thickness [10]. Also, each HDPE layer will attenuate some fraction of incident neutron flux thereby decreasing the incident flux for subsequent converter layers. D.S. McGregor et al. have shown a similar effect in the case of thermal neutron detector with

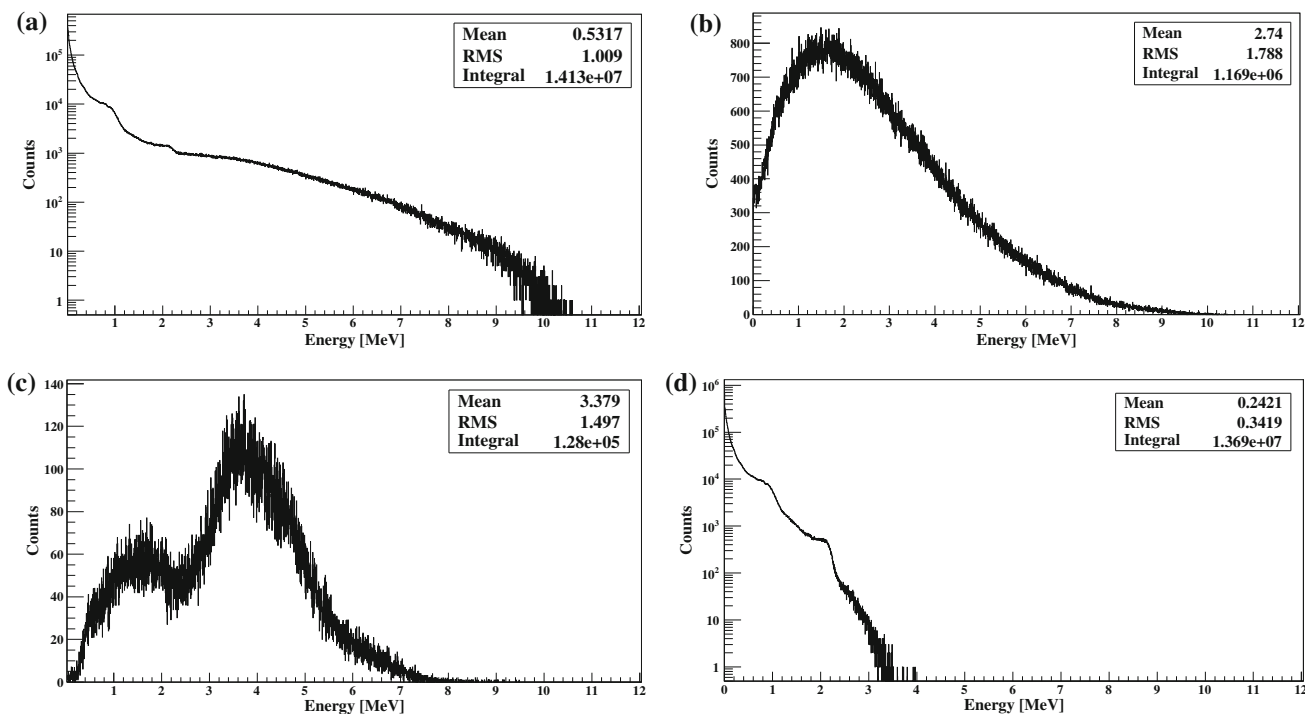


Fig. 6 Energy deposited in SiC by **a** All particles, **b** recoil protons, **c** alphas, and **d** other charged particles

^{10}B and LiF converters [26]. Thus, we can achieve efficiency of up to 1.04% with 10 layers of the stacked detector. Furthermore, the thickness of converter was varied for 5, 10, 15, 20, and 50 stacks, and the maximum efficiency of $\sim 3.85\%$ could be achieved at the converter thickness of around 400 μm . Efficiency for different stacked numbers with respect to converter thickness is represented in Fig. 5b.

Altering the thickness of converter of different layers may help in further enhancing the efficiency, but it is the subject of further detailed study by changing the thicknesses of different layers.

3.7 Calculation of energy deposition

A data analysis framework has been integrated with Geant4 in order to illustrate the contribution of recoil protons, alpha particles, and other charged particles in SiC detector. Figure 6a–d represents the histograms of the total energy deposited, energy deposited by the recoil protons generated in HDPE converter, energy deposited by alpha particles, and energy deposited by other charged reaction products in SiC detector volume, respectively. A LLD of 2 MeV would significantly discriminate the signals due to other charged particles while signals due to α -particles above 2 MeV might provide spurious counts. Furthermore, a discrimination strategy may have to be adopted based on rise time or amplitude to avoid spurious signals. One must

find a suitable balance between LLD setting and detector efficiency as per one's radiation environment.

4 Conclusion

Neutron transport and interaction in SiC detector along with HDPE converter have been investigated using Monte Carlo based Geant4 simulation tool kit. Reactions occurring in HDPE and SiC are tabulated along with their mean energy and frequency. Optimization of the converter layer thickness has been done for different energies of neutrons and a special case of the ^{241}Am -Be neutron source, and it is found to be $\sim 400 \mu\text{m}$. Effect of LLD on SiC detector efficiency was presented, which shows a reduction in efficiency from 0.112% (at LLD of 0 keV) to 0.07% (at LLD of 2 MeV). A stacked detector configuration has been demonstrated to significantly improve the efficiency to 1.04% with 10 layers of stacked detectors and 3.85% with 50 stacked layers. Energy deposition by protons, α , and other charged particles along with total deposition has been demonstrated using ROOT tool. Further investigation is planned to estimate the effect of dead layer and temperature on the efficiency of the single and stacked structure. Also, fabrication of single and stacked detectors will be taken up for a demonstration of improvement in efficiency by comparing the simulated results with experimental results.

Acknowledgements The authors would like to acknowledge Head CD, IGCAR for providing HPC cluster facility to carry out the simulation work. Also, the authors would like to thank Director, IGCAR for providing the opportunity to carry out this study.

References

1. M. Sivaramakrishna, C.P. Nagaraj, K. Madhusoodanan et al., Neutron flux monitoring system in prototype fast breeder reactor. *Int. J. Eng. Innov. Technol.* **3**, 45–53 (2014)
2. N.P. Goldstein, W.H. Todt, A survey of self-powered detectors-present and future. *IEEE Trans. Nucl. Sci.* **26**, 916–923 (1979). doi:[10.1109/TNS.1979.4329746](https://doi.org/10.1109/TNS.1979.4329746)
3. J. Duchene, High temperature fission chambers. *IRE Trans. Nucl. Sci.* **9**, 123–127 (1962). doi:[10.1109/TNS2.1962.4315899](https://doi.org/10.1109/TNS2.1962.4315899)
4. C. Jammes, P. Filliatre, B. Geslot et al., Assessment of the high temperature fission chamber technology for the French fast reactor program. *IEEE Trans. Nucl. Sci.* **59**, 1351–1359 (2012). doi:[10.1109/TNS.2012.2205161](https://doi.org/10.1109/TNS.2012.2205161)
5. W.H. Todt, Characteristics of self-powered neutron detectors used in power reactors, in *Proceedings of a Specialists' Meeting on In-core Inst. and Reactor Core Assessment*, NEA Nuclear Science Committee, 1996
6. V. Verma, C. Jammes, C. Hellesen, P. Filliatre, S. J. Svärd, Feasibility study of self powered neutron detectors in fast reactors for detecting local change in neutron flux distribution. Paper presented at 4th international conference on advancements in nuclear instrumentation measurement methods and their applications (ANIMMA), 2015
7. M. Angelone, A. Kliks, M. Pillon, P. Batistoni, U. Fischer, A. Santagata, Development of self-powered neutron detectors for neutron flux monitoring in HCLL and HCPB ITER-TBM. *Fusion Eng. Des.* **89**, 2194–2198 (2014). doi:[10.1016/j.fusengdes.2014.01.077](https://doi.org/10.1016/j.fusengdes.2014.01.077)
8. G.F. Knoll, *Radiation Detection and Measurement*, 4th edn. (Wiley, New York, 2010)
9. L. Harris Jr., G.F. Knoll, J.S. King, Proton-recoil spectrometer for fast neutron spectra. *Trans. Am. Nucl. Soc.* **8**, 73 (1965)
10. S. Tripathi, C. Upadhyay, C.P. Nagaraj et al., Geant4 simulations of semiconductor detectors (SiC) for fast neutron spectroscopy. Paper presented at annual IEEE India conference (INDICON), New Delhi, India, Dec. 17–20, 2015. doi: [10.1109/INDICON.2015.7443467](https://doi.org/10.1109/INDICON.2015.7443467)
11. R.W. Flammang, J.G. Seidel, F.H. Ruddy, Fast neutron detection with silicon carbide semiconductor radiation detectors. *Nucl. Instrum. Methods A* **579**, 177–179 (2007). doi:[10.1016/j.nima.2007.04.034](https://doi.org/10.1016/j.nima.2007.04.034)
12. K. Sedlačková, B. Zat'ko, A. Šagátová et al., MCNPX Monte Carlo simulations of particle transport in SiC semiconductor detectors of fast neutrons. *J. Instrum.* (2014). doi:[10.1088/1748-0221/9/05/C05016](https://doi.org/10.1088/1748-0221/9/05/C05016)
13. K. Sedlačková, B. Zat'ko, A. Šagátová et al., Monte Carlo simulations of the particle transport in semiconductor detectors of fast neutrons. *Nucl. Instrum. Methods A* (2013). doi:[10.1016/j.nima.2013.01.011](https://doi.org/10.1016/j.nima.2013.01.011)
14. J.A. Dennis, Neutron flux and energy measurements. *Phys. Med. Biol.* **11**, 1 (1966). doi:[10.1088/0031-9155/11/1/301](https://doi.org/10.1088/0031-9155/11/1/301)
15. D.S. McGregor, R.T. Klann, H.K. Gersch et al., Thin-film-coated bulk GaAs detectors for thermal and fast neutron measurements. *Nucl. Instrum. Methods A* **466**, 126–141 (2001). doi:[10.1016/S0168-9002\(01\)00835-X](https://doi.org/10.1016/S0168-9002(01)00835-X)
16. Geant4-A simulation toolkit. <http://geant4.web.cern.ch/geant4/>. Accessed 25 February 2016
17. S. Agostinelli, J. Allison, K. Amako et al., Geant4—a simulation toolkit. *Nucl. Instrum. Methods A* **506**, 250–303 (2003). doi:[10.1016/S0168-9002\(03\)01368-8](https://doi.org/10.1016/S0168-9002(03)01368-8)
18. J. Allison, K. Amako, J. Apostolakis et al., Geant4 developments and applications. *IEEE Trans. Sci.* **53**, 270–278 (2006). doi:[10.1109/TNS.2006.869826](https://doi.org/10.1109/TNS.2006.869826)
19. Geant4 Physics Reference Manual. <http://geant4.web.cern.ch/geant4/G4UsersDocuments/UsersGuides/PhysicsReferenceManual/html/PhysicsReferenceManual.html>. Accessed 25 February 2016
20. ISO 8529-1:2001(en), Reference neutron radiations—Part 1: characteristics and methods of production, <https://www.iso.org/obp/ui/#iso:std:25666:en>. Accessed 15 August 2015
21. Geant4 Reference Physics List. http://geant4.cern.ch/support/proc_mod_catalog/physics_lists/referencePL.shtml. Accessed 25 February 2016
22. F. Franceschini, F.H. Ruddy, in *Silicon Carbide neutron detectors*, ed. by R. Gerhardt. Properties and Applications of Silicon Carbide, (INTECH, 2011). doi: [10.5772/15666](https://doi.org/10.5772/15666)
23. F.H. Ruddy, J.G. Siedel, Effects of gamma irradiation on silicon carbide semiconductor radiation detectors, in *IEEE Nuclear Science Symposium Conference Record*, San Diego, CA, 583–587 (2006). doi: [10.1109/NSSMIC.2006.356223](https://doi.org/10.1109/NSSMIC.2006.356223)
24. James Ziegler - SRIM & TRIM. <http://www.srim.org/>. Accessed 25 February 2016
25. D.S. McGregor, J.K. Shultis, Reporting detection efficiency for semiconductor neutron detectors: a need for a standard. *Nucl. Instrum. Methods A* **632**, 167–174 (2011). doi:[10.1016/j.nima.2010.12.084](https://doi.org/10.1016/j.nima.2010.12.084)
26. D.S. McGregor, M.D. Hammig, Y.H. Yang et al., Design considerations for thin film coated semiconductor thermal neutron detectors—I: basics regarding alpha particle emitting neutron reactive films. *Nucl. Instrum. Methods A* **500**, 272–308 (2003). doi:[10.1016/S0168-9002\(02\)02078-8](https://doi.org/10.1016/S0168-9002(02)02078-8)